Localized Excitation in the Hybridization Gap in $YbAl_3$

A. D. Christianson,[1,2] V. R. Fanelli,[1,2] J. M. Lawrence,[1] E. A. Goremychkin,[3,4] R. Osborn,[3] E. D. Bauer,[2] J. L. Sarrao,[2] J. D. Thompson,[2] C. D. Frost,[4] and J. L. Zarestky[5]

[1]*University of California, Irvine, California 92697, USA*
[2]*Los Alamos National Laboratory, Los Alamos, New Mexico 87545, USA*
[3]*Argonne National Laboratory, Argonne, Illinois 60439, USA*
[4]*ISIS Facility, Rutherford Appleton Laboratory, Chilton, Didcot OX11 0QX, United Kingdom*
[5]*Ames Laboratory, Iowa State University, Ames, Iowa 50011, USA*

(Received 22 April 2005; published 22 March 2006)

The intermediate valence compound $YbAl_3$ exhibits a broad magnetic excitation in the inelastic neutron scattering spectrum with characteristic energy $E_1 \approx 50$ meV, equal to the Kondo energy ($T_K \sim$ 600–700 K). In the low temperature ($T < T_{\mathrm{coh}} \sim 40$ K) Fermi liquid state, however, a new peak in the scattering occurs at $E_2 \approx 33$ meV, which lies in the hybridization gap that exists in this compound. We report inelastic neutron scattering results for a single-crystal sample. The scattering at energies near E_1 qualitatively has the momentum (Q) dependence expected for interband scattering across the indirect gap. The scattering near E_2 has a very different Q dependence: it is a weak function of Q over a large fraction of the Brillouin zone and is smallest near $(1/2, 1/2, 1/2)$. A possibility is that the peak at E_2 arises from a spatially localized excitation in the hybridization gap.

DOI: 10.1103/PhysRevLett.96.117206 PACS numbers: 75.20.Hr, 61.12.Ex, 71.28.+d

The Anderson lattice [1,2], in which a small ($\sim$10–30 meV) gap in the electronic structure arises from hybridization of the $4f$ electrons with the conduction electrons [Fig. 1(f)], is believed to capture the essence of the physics of intermediate valence (IV) compounds. When the Fermi level is in the gap, the behavior is that of the Kondo insulators such as YbB_{12} and SmB_6. The most direct experimental evidence for the gap comes from measurements of the optical conductivity. For example, for YbB_{12} the low temperature conductivity vanishes below 25 meV, and then rises to a maximum in the mid-IR near 0.25 eV [3]. The experimental neutron scattering spectra of the Kondo insulators also show low temperature features whose energy scale is that of the gap. The intensity of these features is highly Q dependent, being smallest at the zone center and peaking at the $(1/2, 1/2, 1/2)$ zone-boundary point in YbB_{12} [4] and SmB_6 [5].

When the Fermi level is not in the gap, the behavior is that of an intermediate valence metal. The cubic (Cu_3Au structure) compound $YbAl_3$ exhibits strong intermediate valence ($z = 2.75$) and a large Kondo temperature ($T_K \sim$ 600–700 K). Below the ''coherence temperature'' $T_{\mathrm{coh}} \sim$ 40 K, where the resistivity exhibits the T^2 behavior expected for a Fermi liquid [6], the optical conductivity exhibits [7] a narrow Drude resonance separated by a deep minimum at 30 meV from a mid-IR peak at 0.25 eV. It is believed that the minimum and the mid-IR peak arise from the (vertical) interband transitions across the hybridization gap, while the Drude resonance arises from intraband transitions across the Fermi level, which lies in a region of high density of states near the zone boundary. Inelastic neutron scattering (INS) experiments [8] in polycrystalline samples of $YbAl_3$ have shown that for $T > 40$ K the magnetic scattering is broad with a characteristic energy of order $E_1 \approx 50$ meV, corresponding to the Kondo temperature, but at low temperature an additional narrow peak occurs in the INS near $E_2 =$ 33 meV. This is the same energy as the minimum in the optical conductivity; i.e., it occurs on the same scale as the hybridization gap. This peak broadens and weakens on alloying with a small concentration of Lu [9], which fact, taken together with the disappearance of the peak above 40 K, means it is a property of the fully coherent ground state.

To explore the physics of this scattering, and, in particular, to determine the Q dependence, we have performed inelastic neutron scattering measurements on single crystals of $YbAl_3$. The crystals were grown by precipitation from excess aluminum (self-flux method). Experiments were performed at 6 and 100 K on the MAPS time-of-flight spectrometer at the ISIS Pulsed Neutron and Muon Facility of the Rutherford Appleton Laboratory. The initial energy was fixed at $E_i = 60$ and 120 meV. Four crystals, of total mass $\sim$5 g, were mounted on an aluminum sample holder and coaligned with a mosaic of 2.5°. We set $\boldsymbol{k_i}$ (the incoming beam wave vector) initially parallel to the $[1, 0, 0]$ direction; in a second set of measurements we chose $\boldsymbol{k_i} \parallel [1, 1, 0]$. Unlike the case of a triple-axis spectrometer where the crystal is rotated to construct a scan over energy transfer with $\boldsymbol{Q} = (2\pi/a_0)\,(h, k, l)$ held constant, for MAPS, where the crystal orientation is fixed during the scan, only three of the four variables h, k, l, and ΔE are independent in any plot at fixed E_i. The scattering was normalized to a vanadium standard and is given in absolute units in Figs. 1–3.

In Fig. 1 we plot the scattering at $T = 6$ K as a function of energy transfer at different momentum transfers. In agreement with the earlier results reported for polycrystals

[8,9], the scattering shows two features: a peak centered at $E_2 = 33$ meV, whose width is essentially equal to the instrumental resolution, and a broad feature centered at $E_1 = 50$ meV. In Figs. 1(a)–1(d) where $k_i \parallel [110]$, both h and k vary with $h + k$ constant, as ΔE varies; in Fig. 1(e) where $k_i \parallel [100]$, only h varies with ΔE. The values of (h, k, l) given in the figure correspond to the values at E_1 and E_2. Since $YbAl_3$ has the Cu_3Au crystal structure (with $a_0 = 4.203$ Å), the Brillouin zone (BZ) is a simple cube centered at Γ and extending ± 0.5 in reduced (h, k, l) units in all three directions. Hence, Fig. 1 shows the E_2 peak at key positions in the BZ, including the Γ point [Fig. 1(a)], various zone-boundary points [Figs. 1(b), 1(d), and 1(e)], and a point in the middle of the BZ [Fig. 1(c)]. Plots at other positions in the BZ are very similar. The variation in the position and the magnitude of the E_2 peak is small. Hence, while the scattering near E_1 shows considerable variation of intensity and line shape with Q, the peak at E_2 appears to be essentially independent of Q.

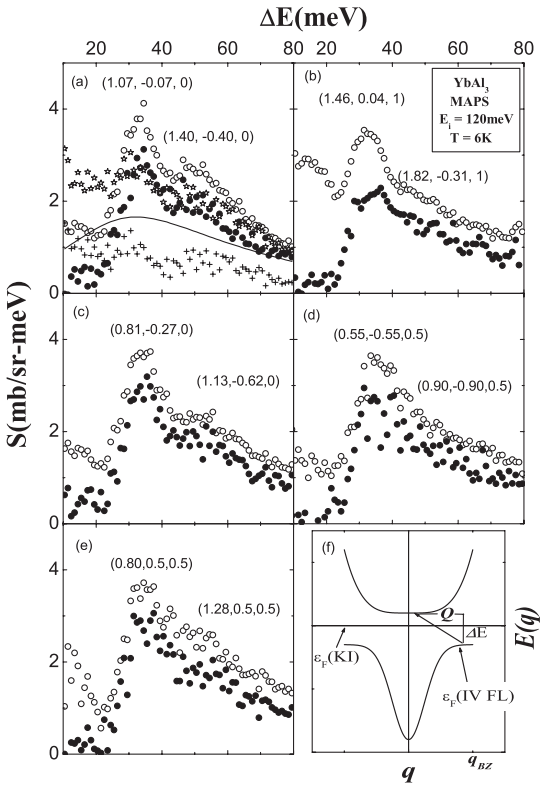

FIG. 1. (a)–(e) The total scattering (open circles) and the magnetic scattering (solid circles) at $T = 6$ K in $YbAl_3$ versus energy transfer at various momentum transfers, measured on MAPS using an initial energy of 120 meV. [Panel (a) also includes the total scattering (stars), nonmagnetic scattering (crosses), and magnetic scattering (line) at 100 K.] The reduced wave vectors given in each panel correspond to the values at $E_1 = 50.5$ meV and $E_2 = 32.5$ meV. Panel (f) shows a schematic plot of the renormalized band structure expected for the Anderson lattice, with a hybridization gap. For IV Fermi liquids (FL), the Fermi level lies in the high density of states region of the lower band; for Kondo insulators (KI), it falls in the gap. A typical interband transition, with energy transfer ΔE and momentum transfer Q, is shown.

Figure 2(a) shows for $k_i \parallel [100]$ an intensity map for the projection onto the k-l plane for an interval of energy transfer $E_1 \pm 5$ meV. In this plot, the reduced wave vector h varies with k and l; contours of constant h are exhibited in the plot. The cubic symmetry is readily apparent. Peaks are observed near $(h, 0.5, 0.5)$, where $h(\Delta E = E_1) = 1.3$. These peaks lie essentially at the zone edge not far from the $(1/2, 1/2, 1/2)$ point. Figure 2(b) shows for $k_i \parallel [100]$ an intensity plot in the $\Delta E - Q_k$ plane for $-0.2 < l < 0.2$. The scattering is basically independent of k for $\Delta E = E_2$; this path traverses the zone center at $(1, 1, 0)$ and the zone boundary at $(0.8, 0.5, 0)$. Figure 2 confirms our observation that the scattering near E_1 is highly Q dependent, peaking at the zone boundary, while the scattering near E_2 is independent of Q.

The total scattering for $\Delta E > 20$ meV decreases with temperature [Fig. 1(a)] and with total Q in the extended zone for $0.4 < l < 2.6$ (not shown here). Hence it cannot

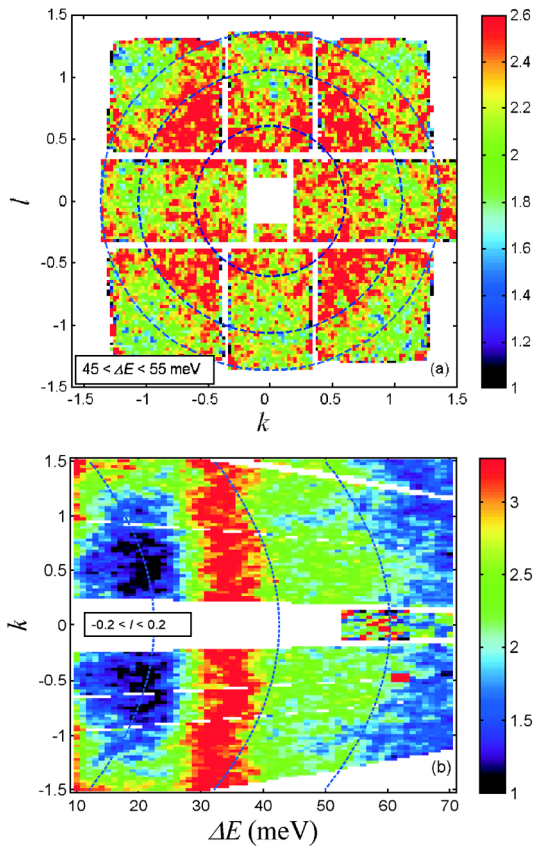

FIG. 2 (color online). (a) Intensity versus reduced wave vector (k, l) for energy transfers in the range $45 < \Delta E < 55$ meV for neutron scattering data taken on $YbAl_3$ at $T = 6$ K, using MAPS with $E_i = 120$ meV. (Circles: contours of constant $h = 1.25, 1.35, 1.45$.) (b) Intensity versus energy transfer ΔE and reduced wave vector k for the component l of reduced wave vector in the range $-0.2 < k < 0.2$. (Parabolas: contours of constant $h = 0.5, 1.0, 1.5$.)

arise from phonon scattering. It does, however, overlap with phonon scattering. To estimate the nonmagnetic scattering we fit the $E_i = 60$ meV data at 100 K to the sum of a q-independent Lorentzian representing the magnetic scattering and three phonon peaks near 12.5, 22, and 30 meV. The best fit gave Lorentzian parameters ($E_0 = 20$ meV and $\Gamma = 40$ meV) similar to those of Ref. [8]. We subtracted the Lorentzian from the scattering to obtain the nonmagnetic scattering at 100 K, scaled the latter to 7 K by the ratio of the thermal (Bose) factors, and subtracted it off to obtain the magnetic scattering at 7 K. Details are shown in Figs. 1(a) and 3(a). The nonmagnetic scattering is quite small for $E_i = 60$ meV; it is larger for $E_i = 120$ meV due to multiple scattering, but remains smaller than the magnetic contribution.

We also measured the spectra on the HB3 triple-axis spectrometer at the High Flux Isotope Reactor (HFIR) at Oak Ridge National Laboratory. Six flux-grown crystals, each approximately 1 g, were coaligned to within $\pm 0.3°$ with the $[1, -1, 0]$ direction vertical. We measured the spectra at 10 and 100 K, using a fixed final energy of 14.7 meV and a collimation 30′-40′-80′-240′. The counting rate is normalized to monitor count units (1 mcu $\approx$ 1 s). For each value of $\boldsymbol{Q_1} = (2\pi/a_0)$ (h, k, l) we measured the 10 K spectra at a second momentum transfer $\boldsymbol{Q_2} = (2\pi/a_0)$ $(h, k, l + 2)$ that is equivalent to $\boldsymbol{Q_1}$ in the reduced zone scheme and has a similar structure factor, and then fit the data as the sum of a magnetic contribution $M(E)$ that varies with Q as the $4f$ form factor and a phonon contribution $Ph(E)$ that scales as Q^2. In Fig. 4(b) it can be seen that at low Q the phonon contribution (solid line) is small compared to the magnetic scattering (open circles), as expected. For comparison we show (solid circles) the magnetic scattering determined using the same method as for the MAPS data. The magnetic scattering obtained by each method is similar, and is similar to that seen in the MAPS data.

In Fig. 4 the $4f$ form factor has been divided out in order to represent the scattering in the reduced zone. The scattering is essentially identical at the zone center, and at the $(0, 0, 1/2)$ and $(1/2, 1/2, 0)$ zone-boundary points. This confirms our time-of-flight result that the 30 meV scattering is largely Q independent. We note, however, that the scattering at the $(1/2, 1/2, 1/2)$ zone-boundary point is considerably weaker. This effect can also be seen in the time-of-flight data in Fig. 3(c) and to a lesser extent in Fig. 1(d).

Our basic result, then, is that the scattering near $E_1 = 50$ meV is highly Q dependent, with peaks at the $(1/2, 1/2, 1/2)$ zone boundary, but apart from the variation with the $4f$ form factor, the scattering near $E_2 = 33$ meV appears to be only weakly dependent on Q, being strongest

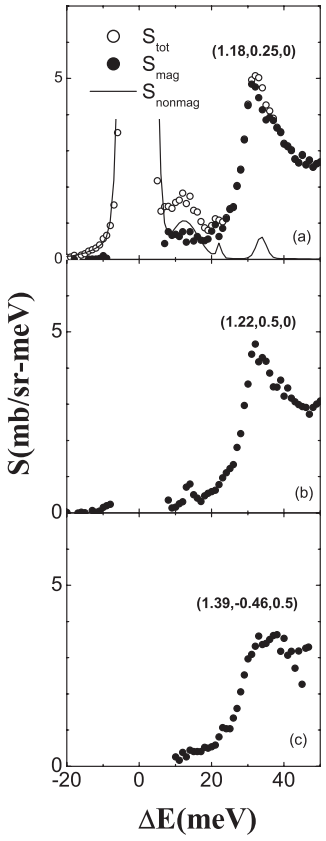

FIG. 3. The magnetic scattering (solid circles) versus energy transfer measured on MAPS at 7 K using $E_i = 60$ meV. The reduced wave vector given in each panel corresponds to the value at $\Delta E = 32.5$ meV. [The open circles in (a) are the total scattering; the solid line is the nonmagnetic scattering.]

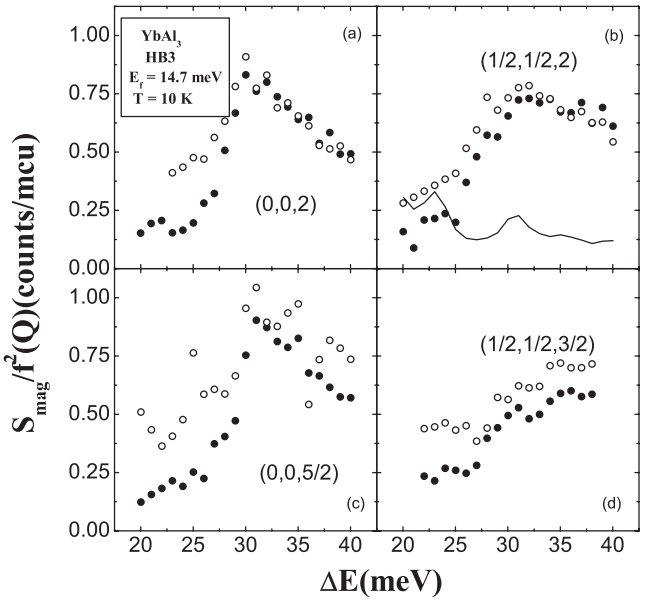

FIG. 4. The magnetic contribution to the scattering of $YbAl_3$ at $T = 10$ K and at four values of momentum transfer $\boldsymbol{Q} = 2\pi/a_0$ (h, k, l). The data have been divided by the $4f$ form factor, and thus represent the scattering in the reduced zone. The magnetic scattering was determined by subtracting phonons determined (1) at 10 K by Q^2 scaling (open circles) and (2) at 100 K by assuming a Lorentzian for the magnetic scattering (solid circles). An example of the phonons is given in (b) as a solid line.

near the zone center and weakest near the $(1/2, 1/2, 1/2)$ point.

In calculations [1,2] of the interband transitions in the renormalized band structure [Fig. 1(f)] of the Anderson lattice, the scattering is highly Q dependent. The most intense scattering occurs when the energy transfer ΔE equals the threshold for indirect transitions between the regions of large density of states at the zone center and the zone boundary of the upper and lower bands, respectively. This occurs when $Q = q_{\mathrm{BZ}}$ [Fig. 1(f)]. At smaller Q, the scattering is weaker and occurs at higher energy. When the Fermi level does not lie in the gap, so that the behavior is that of an IV metal, the interband transitions still occur and show a very similar Q dependence to that of the Kondo insulators (see Fig. 5 of Ref. [1]). In addition, low energy intraband scattering across the Fermi surface is expected; this is related to the Drude scattering in the optical conductivity. The characteristic energy for such scattering varies linearly with Q, as expected on general grounds for a Fermi liquid.

In $YbAl_3$ the scattering near $E_1 = 50$ meV shows considerable Q dependence and peaks near the $(1/2, 1/2, 1/2)$ zone-boundary point, consistent with interband scattering across an indirect gap of order 50 meV. We note that this is also the Kondo scale for this compound; if so, the high temperature Kondo scattering evolves into interband scattering with the same energy scale.

Sharp excitations at low temperatures, whose energy scale is that of the hybridization gap, have been observed at low temperatures in the Kondo insulators SmB_6 [5], YbB_{12} [4], and TmSe [10]. These excitations are highly Q dependent. For example, in TmSe the intensity is at least a factor of 4 smaller at zone center than at the zone boundary, and in YbB_{12} and SmB_6 the intensity is largest at the zone boundary along the $[1, 1, 1]$ direction, decreasing dramatically as Q increases or as the angle of $\boldsymbol{Q}$ with respect to the $[1, 1, 1]$ direction changes. Such scattering thus has the behavior expected for threshold scattering at the zone boundary.

By contrast, the sharp E_2 peak in $YbAl_3$ shows little variation in intensity for different values of $\boldsymbol{Q}$ that include the zone center, key zone-boundary points, and points in the center of the reduced zone (Figs. 1 and 4); and in addition the scattering is *weaker* at the $(1/2, 1/2, 1/2)$ point [Figs. 3(c) and 4(d)]. Hence the Q dependence of this excitation is *opposite* to what is seen in the Kondo insulators. It clearly does not have the Q dependence expected for threshold interband scattering, unless the actual renormalized band structure is very different from that shown in Fig. 1(f). This excitation occurs at too large an energy, and lacks the expected Q dependence, to arise from intraband Fermi surface scattering. Since the amplitude of this peak is strongly diminished at 100 K, it cannot represent a crystal field transition; and, indeed, well-defined crystal field excitations are not expected in intermediate valence systems with such large Kondo temperatures. The magnetic scattering at E_2 *may* arise from coupling to the optic phonon which is seen at nearly the same energy.

An important possibility is that the scattering represents a spatially localized excitation. The energy of the excitation coincides with the deep minimum in the optical conductivity; this suggests that the localized excitation lies inside the hybridization gap, having the character of an exciton. Riseborough [11] showed that a magnetic bound state, whose energy lies below the interband threshold, can arise in the Kondo insulators due to RKKY interactions. Such a bound state, however, should be large for zone-boundary Q, dispersing and losing amplitude rapidly as Q decreases. Brandow [2] postulated the existence of a localized on-site valence fluctuation from the hybridized state into the unhybridized trivalent ($4f^{13}$) state. He showed that when such an elementary excitation, which unbinds or unscreens a local moment, is included in a consistent manner with the usual excited states of the Anderson lattice, a two-peak structure of the susceptibility and specific heat should occur, similar to the low temperature anomalies observed [6] experimentally in $YbAl_3$. In his treatment, however, the excitation was not derived from the Anderson lattice Hamiltonian but was included in an *ad hoc* manner. It is thus an open question of whether and how such an excitation can arise in the context of the Anderson lattice. It is also unclear why a local excitation should be so sensitive to alloy disorder [9].

We are grateful to Steve Shapiro for sharing and discussing his unpublished data on this compound, and to Peter Riseborough and Steve Nagler for helpful discussions. Work at UC Irvine was supported by the U.S. Department of Energy (DOE) under Grant No. DE-FG03-03ER46036. Work at Argonne National Laboratory was supported by the DOE under Contract No. W-31-109-ENG-38. Ames Laboratory is supported by DOE Contract No. W-31-109-ENG-38. Work at HFIR was supported by DOE Contract No. DE-AC05-00OR22725. Work at Los Alamos National Laboratory was also performed under the auspices of the DOE.

[1] A. A. Aligia and B. Alascio, J. Magn. Magn. Mater. **46**, 321 (1985).
[2] B. H. Brandow, Phys. Rev. B **37**, 250 (1988).
[3] H. Okamura *et al.*, Phys. Rev. B **58**, R7496 (1998).
[4] J.-M. Mignot *et al.*, Phys. Rev. Lett. **94**, 247204 (2005).
[5] P. A. Alekseev *et al.*, J. Phys. Condens. Matter **7**, 289 (1995).
[6] A. L. Cornelius *et al.*, Phys. Rev. Lett. **88**, 117201 (2002).
[7] H. Okamura *et al.*, J. Phys. Soc. Jpn. **73**, 2045 (2004).
[8] A. P. Murani, Phys. Rev. B **50**, 9882 (1994).
[9] R. Osborn *et al.*, J. Appl. Phys. **85**, 5344 (1999).
[10] S. M. Shapiro and B. H. Grier, Phys. Rev. B **25**, 1457 (1982).
[11] P. S. Riseborough, Ann. Phys. (Berlin) **9**, 813 (2000).